ISSN 2616-5767 Vol.9, Issue 3: 1-14, DOI: 10.25236/AJETS.2026.090301

# Multi-Scale Simulation of $Al_2O_3$ Particle Formation and Evolution during Aluminum Particle Group Combustion Using a Coupled CFD–PBE–TEMOM Model

**Ningning Sun[1,a,*], Bingfa Zhang[1,b], Ya Jiang[2,c]**

[1]*College of Science, China Jiliang University, Hangzhou, 310018, China*
[2]*College of Science, China Jiliang University, Hangzhou, 310018, China*
[a] *austsnn@163.com*
** Corresponding author*

***Abstract:*** *Aluminum powder as an important high-energy additive in solid propellants, can significantly improve propellant specific impulse. However, the large amount of aluminum oxide particles produced during its combustion can easily cause nozzle deposition and two-phase flow losses, affect engine performance. Regarding the problem of the difficulty in accurately predicting the formation and evolution of alumina particles during the combustion of aluminum particle clouds, this paper constructs a numerical model that couples the Euler–Lagrange two-phase flow framework with the Population Balance Equation (PBE), and use the Taylor Expansion Matrix Method (TEMOM) to achieve efficient solving of PBE, thus achieving a quantitative prediction of the evolution of alumina particle size distribution. Numerical simulation of the jet combustion process of aluminum particles with different particle sizes of 200 nm, 400 nm, and 600 nm, analyzed the temperature structure of the flow field and the evolution pattern of alumina particles. The results show that smaller aluminum particles ignite earlier and burn more rapidly, as the particle size increases, the temperature peak moves downstream along the axis. The number density of alumina particles along the axial direction shows a distribution feature of first increasing and then decreasing, the geometric standard deviation of its volume eventually stabilizes at about 1.8–2.0,exhibits typical self-preserving distribution characteristics. The research results can provide a theoretical basis for optimizing the particle size of propellant aluminum powder and inhibiting engine deposits.*

***Keywords:*** *Aluminum oxide particles; Euler–Lagrange two-phase flow; Population Balance Equation (PBE); Taylor Expansion Matrix Method (TEMOM)*

## 1. Introduction

Solid propellants are the core power source in the fields of aerospace, military, and deep space exploration. In recent years, with the rapid development of near-Earth space resource exploitation, deep space exploration, and missile weapon systems, there have been stringent requirements for the energy performance, combustion stability, and environmental adaptability of solid propellants. To meet the diverse demands of tasks, propellants not only need to have characteristics such as high energy density, low cost, and non-toxicity, but should also possess the advantage of being widely sourced. Metallic aluminum powder, due to its extremely high volumetric calorific value and mass combustion enthalpy, has become a core additive for improving the specific impulse of solid propellants and has been widely used in aerospace, military, and civilian fields.

The addition of aluminum particles [1-2] can significantly enhance the energy level of propellants, but the aluminum oxide particles produced during combustion can cause non-negligible two-phase flow problems [3-5]. These oxide particles form solid products in the combustion chamber, leading to increased turbulence and flow resistance, and they deposit on the nozzle and walls, severely limiting the performance and reliability of the engine. Therefore, accurately predicting the formation, evolution, and size distribution of alumina particles is of significant engineering value for optimizing propellant formulations and suppressing deposition. The study of the combustion mechanism of aluminum particles began in the 1950s. Early research mainly drew on the combustion models of hydrocarbon fuel droplets, treating aluminum particle combustion as a gas-phase diffusion flame-controlled process. At the single-

ISSN 2616-5767 Vol.9, Issue 3: 1-14, DOI: 10.25236/AJETS.2026.090301

particle scale, Altman and Pantoya [6] pointed out in their latest review that accurately simulating the combustion of aluminum particles requires considering three key physical phenomena: the boiling at the alumina-aluminum particle interface, the condensation loss during the formation of alumina nanoparticles, and the heat transfer mechanism on the particle surface. Finke [7] proposed a comprehensive population balance model framework that takes into account multiple physical processes such as nucleation, condensation, evaporation, and coalescence, successfully predicting the evolution of alumina particles during the combustion of a single aluminum particle. The review study by Ben Moussa [8] and others indicates that at the scale of particle populations, the combustion mechanism of single particles is fairly well understood, but the ignition conditions, combustion patterns, and flame propagation speed in particle population combustion still require more research. Therefore, this article will study the combustion of particle clusters.

The development of Computational Fluid Dynamics (CFD) [9] provides a powerful tool for addressing the aforementioned issues. In recent years, researchers have begun using the Euler-Lagrange framework to simulate the combustion behavior of aluminum particle clusters. For example, an analysis framework for the combustion of micron-sized aluminum droplets in solid rocket engines was established using the Euler-Lagrange coupling method [10], studying the effect of droplet size distribution on combustion. Zhu et al. [11-12] also developed a computational solver based on the Euler-Lagrange model to study the effect of adding aluminum powder to the afterburner combustion process in solid fuel ramjet engines.

This study established a multiscale numerical model by coupling an Euler-Lagrange framework with the population balance equation-Taylor expansion moment method (PBE-TEMOM) [13-14] solver, developing a computational method capable of predicting the particle size distribution of alumina during the combustion process of aluminum particles, and revealing its evolution regularity. The remaining content of this paper is organized as follows. Section two presents the numerical methods for the gas phase and particle phase control equations, as well as the combustion model of aluminum particles. Section three introduces the computational setup, grid independence analysis, and model validation. The results and discussion are provided in Section four. Section five summarizes the entire text.

## 2. Governing Equations and Multi-Physics Coupled Model

The physical processes involved in this study span multiple time and spatial scales, including macroscopic turbulent gas-phase flow fields, the forces on and combustion evaporation of aluminum particles, and the nucleation and coagulation growth of nano aluminum oxide (Al2O3) particles. For this purpose, this paper establishes a set of strongly coupled multiphase dynamic models.

### *2.1. Gas Phase*

The gas phase is treated as a compressible reacting fluid. Based on the conservation laws, considering the source terms of the particulate phase, the transport equations for continuity, momentum, energy, and species mass fractions can be expressed as:

(1) Continuity equation:

$$\frac{\partial \rho}{\partial t}+\frac{\partial}{\partial x_j}\left(\rho u_j\right)=S_m \tag{1}$$

Here, $t$ is time, $\rho$ is density, and $S_m$ is the mass source term, which comes from the mass of aluminum vapor released during the evaporation or combustion of aluminum particles, calculated using the Lagrangian particle tracking method:

$$S_m=-\frac{1}{V_{cell}}\sum_{particles}\frac{dm_p}{dt} \tag{2}$$

Here, $m_p$ is the mass evaporation rate of a single particle, and $V_{cell}$ is the volume of the grid cell.

(2) Momentum conservation equation:

$$\frac{\partial(\rho \mathrm{u})}{\partial t}+\nabla\cdot(\rho \mathrm{uu})=-\nabla p+\nabla\cdot\tau+S_p \tag{3}$$

Here, $S_p$ is the momentum source term exerted by the discrete phase particles on the gas phase.

ISSN 2616-5767 Vol.9, Issue 3: 1-14, DOI: 10.25236/AJETS.2026.090301

Where $\tau$ is the stress tensor, and the expression is:

$$\tau = \mu\left(\nabla \mathrm{u} + \nabla \mathrm{u}^T - \frac{2}{3}(\nabla \cdot \mathrm{u})\mathrm{I}\right) \tag{4}$$

(3) Energy conservation equation:

$$\frac{\partial(\rho h)}{\partial t} + \nabla \cdot (\rho u h) = \nabla \cdot (k \nabla T) + \sum_i h_i \, \dot{\omega}_i + S_h \tag{5}$$

Here,$h$ is the specific enthalpy of the gas-phase mixture, $\dot{\omega}_i$ is the net generation rate of chemical reactions of component i, and $S_h$ includes the heat released by the combustion of aluminum particles and the convective heat transfer between phases.

(4) Component transport equation:

$$\frac{\partial(\rho Y_i)}{\partial t} + \nabla \cdot (\rho \mathrm{u} Y_i) = \nabla \cdot (\rho D_i \nabla Y_i) + \dot{\omega}_i + S_{i,p} \tag{6}$$

Here, $Y_i$ and $D_i$ are the mass fraction and effective diffusion coefficient of component i, respectively, and $S_{i,p}$ is the coupling term of mass transfer between particles and the gas phase.

### *2.2. Granular Phase*

Aluminum particles are tracked in terms of their motion, heat transfer, evaporation, and combustion behavior using a Lagrangian framework as the discrete phase. Each aluminum particle is considered a point mass, and its movement and evolution in the Eulerian flow field are achieved by solving the following governing equations.

The motion of aluminum particles is described by Newton's second law, solving separately for their position and velocity changes:

(1) Trajectory equation:

$$\frac{d\overrightarrow{X_p}}{dt} = \overrightarrow{V_p} \tag{7}$$

Here, $X_p$ is the particle position, and $V_p$ is the particle velocity.

(2) Velocity equation:

$$\frac{d\overrightarrow{V_p}}{dt} = \frac{\overrightarrow{F_D}}{m_p} + \vec{g} + \overrightarrow{F_{\text{other}}} \tag{8}$$

Here, $m_p$ is the particle mass, $V_p$ is the gravitational acceleration, $g$ is the gravity term, and $F_{\text{other}}$ includes other possible forces (such as virtual mass force, pressure gradient force, etc., which are neglected in this study). The main acting force is the aerodynamic drag $F_D$.

(3) Drag force model (using the Schiller-Naumann model):

$$\overrightarrow{F_D} = \frac{18\mu}{\rho_p d_p^2}\frac{C_D Re_p}{24}\left(\vec{V} - \overrightarrow{V_p}\right) \tag{9}$$

Where $V$ is the local airflow velocity, $d_p$ is the particle diameter, $\rho_p$ is the particle density, and $Re_p$ is the particle Reynolds number, defined as:

$$Re_p = \frac{\rho d_p \left|\vec{V} - \overrightarrow{V_p}\right|}{\mu} \tag{10}$$

The drag coefficient $C_D$ is calculated using the Schiller-Naumann formula:

$$C_D = \begin{cases} \frac{24}{Re_p}\left(1 + \frac{1}{6}Re_p^{2/3}\right), Re_p \le 1000 \\ 0.44, Re_p > 1000 \end{cases} \tag{11}$$

ISSN 2616-5767 Vol.9, Issue 3: 1-14, DOI: 10.25236/AJETS.2026.090301

### *2.3. Homogeneous Nucleation Kinetics of $Al_2O_3$*

When the concentration of $Al_2O_3$ vapor generated in the gas phase exceeds its saturated vapor pressure, the system will form primary nanoparticles through homogeneous nucleation. According to classical nucleation theory, the nucleation rate $J$ is:

$$J = Z\beta n_1 \exp\left(-\frac{\Delta G^*}{k_B T}\right) \tag{12}$$

Here, $Z$ is the Zeldovich factor, $\beta$ is the monomer collision frequency, and $n_1$ is the concentration of monomers in the gas phase. The nucleation barrier $\Delta G^*$ and the critical nucleus volume are given by:

$$\Delta G^* = \frac{16\pi\sigma^3 v_m^2}{3(k_B T \ln S)^2} \tag{13}$$

$$v^* = \frac{32\pi\sigma^3 v_m^3}{3(k_B T \ln S)^3} \tag{14}$$

The newly formed critical nuclei will be introduced as source terms into the nanoparticle dynamics model.

### *2.4. Nanoparticle Evolution and TEMOM Closure*

During the combustion of aluminum particles, the alumina particles produced in the gas-phase reactions undergo transport and collision coagulation in the turbulent flow field, and their particle size distribution continuously evolves over time and space. To describe the kinetic behavior of a polydisperse population of alumina particles, a population balance equation (PBE) is introduced to model the particle number density function $n(v,t)$. In this paper, considering only aggregation, condensation, and nucleation processes, the population balance equation can be expressed as:

$$\frac{\partial n(v,t)}{\partial t} = \left\{\frac{1}{2}\int_{v_{\min}}^{v_{\max}} \beta\,(v-u,u,t)n(v-u,t)n(u,t)du - n(v,t)\int_{v_{\min}}^{V\max} \beta\,(v,u,t)n(u,t)du\right\}_{coa}$$

$$-\left\{\frac{\partial(G(v,t)n(v,t))}{\partial v}\right\}_{con} + \{J(v,t)\delta(v_{nul},v)\}_{nuc} \tag{15}$$

Since the alumina particles generated in this paper are extremely small in size, their coagulation process falls into the free molecular regime, hence the free molecular regime Brownian coagulation kernel is used:

$$\beta(v,v') = B_1\left(\frac{1}{v}+\frac{1}{v'}\right)^{1/2}(v^{1/3}+v'^{1/3})^2 \tag{16}$$

In the formula,$B_1 = \left(\frac{3}{4\pi}\right)^{1/6}\left(\frac{6k_BT}{\rho_p}\right)^{1/2}$, $k_B$ is the Boltzmann constant, $T$ is the gas temperature, and $\rho_p$ is the particle density.Due to the highly nonlinear double integral in the PBE, directly solving it is extremely computationally expensive.Therefore, the moment method is introduced, converting the PBE into the solution of a finite number of particle volume moments $M_k$. The k order moment is defined as:

$$M_k = \int_0^\infty v^k\, n(v)dv \quad (k = 0,1,2) \tag{17}$$

Here, $M_0$ represents the particle number density, $M_1$ represents the total volume concentration, and $M_2$ reflects the width of the particle size distribution. Multiplying both sides of the PBE by $v^k$ and integrating over all volumes yields the unclosed moment transport equation:

$$\frac{\partial M_k}{\partial t} = \left(\frac{\partial(GM_k)}{\partial v}\right)_{con} + Jv^{*k} + \left(\frac{\partial M_k}{\partial t}\right)_{coa} \tag{18}$$

Due to the complex fractional-order characteristics of the coagulation nuclei in the free molecular region, the above moment equations cannot be directly closed using a finite number of integer-order moments. This paper uses the Taylor Expansion Moment Method (TEMOM) proposed by Mingzhou Yu and others to close the coalescence source term. The core idea of TEMOM is not to assume the particle

ISSN 2616-5767 Vol.9, Issue 3: 1-14, DOI: 10.25236/AJETS.2026.090301

size distribution form of the particle population in advance, but to expand the coagulation kernel in a Taylor series at the average particle volume $u = M_1/M_0$.

According to the derivation by Yu et al., by truncating the first three terms of the Taylor expansion, the fractional condensation integral can be completely transformed into an algebraically closed form composed of $M_0$, $M_1$, and $M_2$.Substitute the closed source terms into the moment transport equation to obtain the final set of moment control equations:

Zeroth-order moment (number density) transport equation:

$$\frac{\partial M_0}{\partial t} = \left(\frac{\partial (GM_0)}{\partial v}\right)_{con} + J + \frac{\sqrt{2}B_1(65M_2^2M_0^{23/6} - 1210M_2M_1^2M_0^{17/6} - 9223M_1^4M_0^{11/6})}{5184M_1^{23/6}} \tag{19}$$

First-order moment (volume concentration) transport equation:

$$\frac{\partial M_1}{\partial t} = \left(\frac{\partial (GM_1)}{\partial v}\right)_{con} + \left(\frac{\partial M_1}{\partial t}\right)_{con} + Jv^* \tag{20}$$

Second-order moment (distribution width) transport equation:

$$\frac{\partial M_2}{\partial t} = \left(\frac{\partial (GM_2)}{\partial v}\right)_{con} + Jv^{*2} + \frac{\sqrt{2}B_1(701M_2^2M_0^{11/6} - 4210M_2M_1^2M_0^{5/6} - 6859M_1^4M_0^{-1/6})}{2592M_1^{11/6}} \tag{21}$$

### *2.5. Aluminum Particle Combustion Model*

This paper studies nanoscale particles, with the heat transfer process between the particles and the gas phase considered through the transition state or free molecular state equations. According to the experimental results of Bazyn et al. [15], the combustion process of nanoscale aluminum particles occurs in the condensed phase, dominated by chemical kinetics. Therefore, the combustion reaction of nanoscale aluminum particles can be regarded as a heterogeneous surface reaction. According to the studies of Zou et al. [16-17], the convective models for the continuum state, free molecular state, and transition state are expressed as:

$$\dot{q}_{\mathrm{con-Cm}} = \pi Nu D_{\mathrm{p}} \lambda_{\mathrm{a}}^* \left(T_{\mathrm{a}} - T_{\mathrm{p}}\right), \quad Kn \le 0.01 \tag{22}$$

$$\dot{q}_{\mathrm{con-Fm}} = \frac{1}{8}\pi\alpha D_{\mathrm{p}}^2 P_{\mathrm{a}} \sqrt{\frac{8k_{\mathrm{B}}T_{\mathrm{a}}}{\pi m_{\mathrm{a}}}} \left(\frac{\gamma^* + 1}{\gamma^* - 1}\right) \frac{T_{\mathrm{r}} - T_{\mathrm{p}}}{T_{\mathrm{a}}} N_{\mathrm{Fm}}(T_{\mathrm{a}}, V_{\mathrm{r}}), \quad 10 < Kn \tag{23}$$

$$\frac{1}{\dot{q}_{\mathrm{con-Tran}}} = \frac{1}{\dot{q}_{\mathrm{con-Cm}}} + \frac{1}{\dot{q}_{\mathrm{con-Fm}}}, \quad 0.01 < Kn \le 10 \tag{24}$$

Among them, $Nu$ is the average surface cell number, $\alpha$ is the thermal adjustment coefficient,$k_{\mathrm{B}}$ is the Boltzmann constant, and $T_{\mathrm{a}}$, $T_{\mathrm{p}}$, and $T_{\mathrm{r}}$ are the ambient temperature, gas temperature, and recovery temperature, respectively.

Aluminum consumption rate during the combustion phase:

$$\frac{dm_{\mathrm{Al}}}{dt} = S_{\mathrm{rea}} M_{\mathrm{Al}} [A \exp(-E_{\mathrm{a}}/RuT_{\mathrm{a}})] P_{\mathrm{a}} X_{\mathrm{O_2}} \tag{25}$$

Among them, $S_{\mathrm{rea}}$ is the surface area of aluminum particles, $M_{\mathrm{Al}}$ is the molecular weight of aluminum particles, and $X_{\mathrm{O_2}}$ is the molar mass of oxygen in the mixture.

According to the consumption rate of aluminum, the heat release rate can be calculated as:

$$\dot{q}_{\mathrm{hsr}} = h_{\mathrm{r}} \frac{dm_{\mathrm{Al}}}{dt} \tag{26}$$

Here,$h_{\mathrm{r}}$= $4 \times 10^{-7}$ J/kg, which is the amount of heat released per unit mass of aluminum.

ISSN 2616-5767 Vol.9, Issue 3: 1-14, DOI: 10.25236/AJETS.2026.090301

## 3. Calculation Settings and Model Verification

### *3.1. Geometric Models and Meshes*

The burner geometry model used in this study is shown in Figure 1. It is an axisymmetric structure, consisting of a central fuel inlet and a surrounding annular oxidizer inlet. Aluminum particles are delivered into the combustion chamber by a carrier gas (inert gas) through a circular tube with a central diameter of 10 mm, while high-temperature co-flowing air is introduced into the surrounding annular region as the oxidizer. This structure can effectively simulate the ejection and combustion environment of aluminum particles in actual solid rocket engines, while also facilitating the implementation of symmetric boundary conditions to simplify calculations.

To verify the independence of the simulation results from the mesh, this study conducted a mesh independence analysis. Three different mesh densities (coarse, medium, and fine) were set, with the number of meshes being approximately 100,000, 150,000, and 200,000, respectively. Compared the temperature distribution along the center axis of the burner and the distributions of alumina particle number density and velocity under three different grids. The results are shown in Figure 2, where the difference between the calculations of the medium and fine grids is less than 2%, while there is a significant deviation between the coarse and medium grids. Considering both computational accuracy and efficiency, a medium mesh was ultimately chosen for all subsequent simulations. The grid was locally refined in the combustion reaction zone to ensure high-resolution capture of the flame structure and particle evolution process.

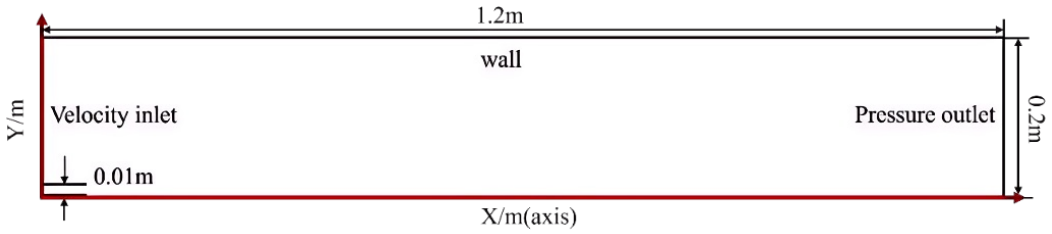


*Figure 1: Simulation mesh images.*

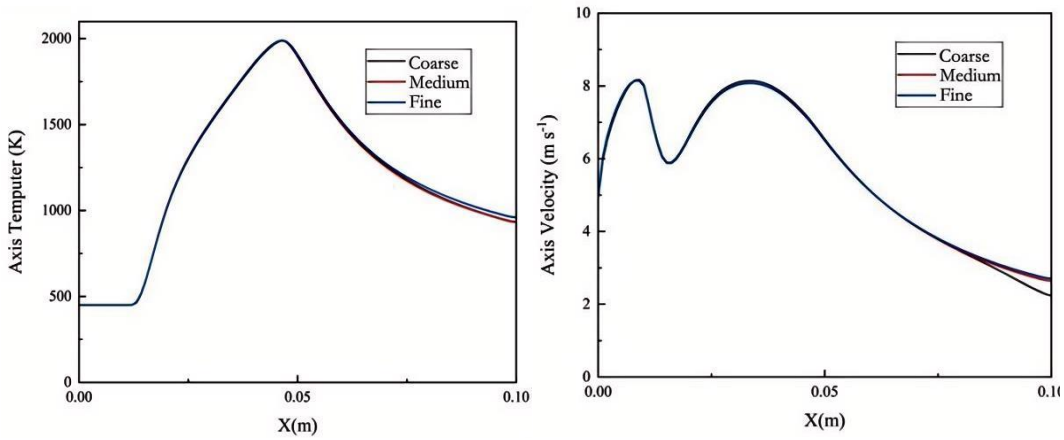


*(a)Temperature* *(b)Velocity*

ISSN 2616-5767 Vol.9, Issue 3: 1-14, DOI: 10.25236/AJETS.2026.090301

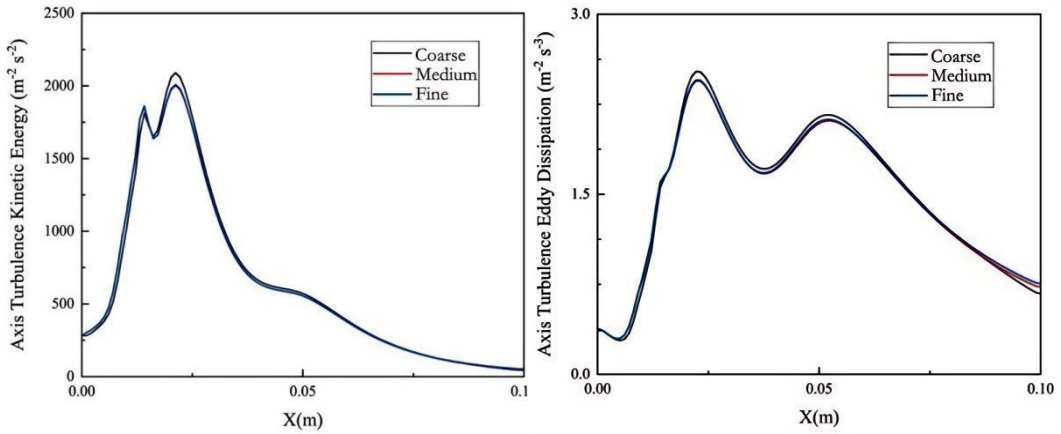


*(c)Kinetic energy* *(d)Vortex dissipation*

*Figure 2: Comparison chart of parameters for different grid axes.*

### *3.2. Boundary Conditions and Initial Conditions*

To accurately simulate the combustion behavior of aluminum particles in a high-temperature oxidative environment, this study set the following physical conditions for each boundary of the computational domain, with all settings referring to the typical operating conditions of aluminum powder combustion in actual solid rocket engines and relevant literature data. At the inlet of the particle-air mixture, the velocity is set to 10 m/s, the initial temperature is 1000 K, the carrier gas is N2, and aluminum particles with diameters of 200 nm, 400 nm, and 600 nm are simulated, assuming that the aluminum particles are all spherical in shape. At the co-flow inlet, set a mixed gas with a composition of 23% $O_2$and 77% $N_2$, an inlet velocity of 5 m/s, and an initial temperature of 2300 K. Use a pressure outlet condition at the domain exit, with a gauge pressure of 0 Pa, and set to prevent backflow. The wall boundaries use no-slip, adiabatic, and smooth boundary conditions, while the central axis applies axisymmetric boundaries to simplify the calculation process. During the initialization of the computational domain, the air is filled with an internal pressure of 101325 Pa (1 atm) and a temperature of 300 K, with the initial flow velocity set to 0 m/s, aluminum particles are uniformly injected into the flow field from the central jet inlet.

### *3.3. Model Validation*

To verify the predictive capability of the numerical model in this paper for the structure of aluminum particle-air jet flames, the radial distributions of temperature at different axial positions obtained from the calculations are compared with the results in the literature by Xiangrui Zou et al. [18]. Figure 3(a) shows the radial temperature distribution curves calculated in this paper at axial positions X = 5 mm, 15 mm, 30 mm, and 80 mm, while Figure 3(b) presents the corresponding results from the literature. From the comparison, it can be seen that the two show good consistency in both the temperature distribution pattern and the evolution trend: near the nozzle (X = 5 mm), the temperature exhibits a sharp single-peak shape, indicating that the combustion reaction has not yet fully developed; as the axial distance increases to X = 15 mm, the temperature peak significantly rises and migrates outward; at X = 30 mm, the temperature distribution becomes more gradual, and the reaction zone further expands; at the downstream position of X = 80 mm, the radial temperature distribution presents a typical parabolic shape. The above comparison verifies that the model in this paper can accurately capture the structural evolution characteristics of the flame during aluminum particle combustion, providing a reliable flow field basis for the subsequent analysis of the formation and agglomeration behavior of alumina particles.

ISSN 2616-5767 Vol.9, Issue 3: 1-14, DOI: 10.25236/AJETS.2026.090301

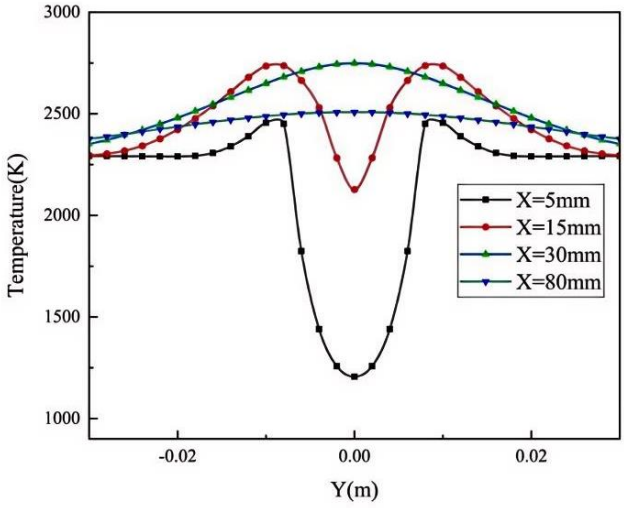


*(a)*

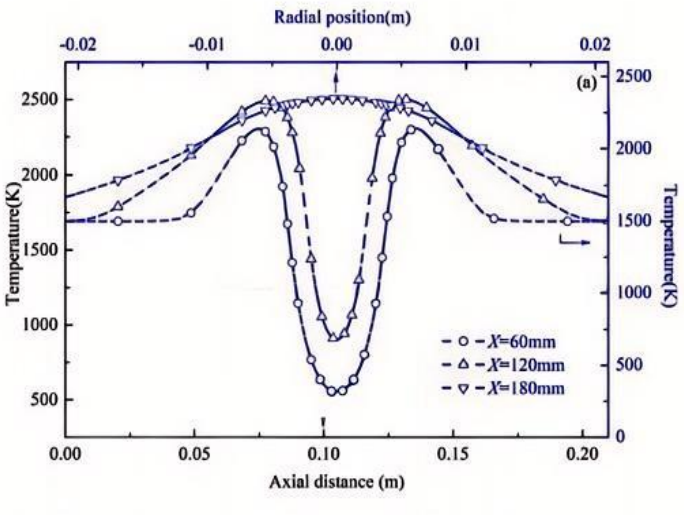


*(b)*

*Figure 3: Radial temperature distribution diagram.*

## 4. Results and Discussion

### *4.1. Gas Phase*

Figure 4 shows the distribution cloud map of the mass fractions of key gas-phase components in the flow field after the combustion of aluminum particles reaches a stable state. To systematically reveal the impact of particle size on combustion characteristics, this paper selects three characteristic particle sizes of 200 nm, 400 nm, and 600 nm for numerical simulation, covering a range from nanoscale to submicroscale. The mass flow rate of aluminum particles is kept constant under all working conditions to ensure the comparability of gas phase component distribution. Although under the same mass flow rate, the distribution pattern of gas-phase components corresponding to different particle sizes is generally similar, the difference in particle size can change the particle number concentration and specific surface area, thereby affecting the heat absorption rate, evaporation rate, and the amount and distribution range of gas-phase components released. Therefore, this paper takes 400 nm particles as a representative and analyzes in detail the spatial distribution characteristics of each component in the flow field, as shown in Figure 4(a)~(f).

As can be seen from Figure 4(b), gaseous aluminum is concentrated in the core region of the jet. After aluminum particles are sprayed into the flow field, they absorb heat from the high-temperature air and rapidly heat up to the evaporation temperature, beginning to evaporate and release gaseous aluminum. The distribution of gaseous aluminum reaches its peak concentration at X = 0.2 m, and then gradually

ISSN 2616-5767 Vol.9, Issue 3: 1-14, DOI: 10.25236/AJETS.2026.090301

decreases along the axial direction. Outside the region where gaseous aluminum is distributed, suboxide components such as AlO, $Al_2O$, AlO, and $Al_2O_2$are distributed in sequence, as shown in Figure 4(c)~(f). These suboxides are all formed during the gas-phase combustion process of aluminum particles. Because aluminum combustion involves complex multi-step chemical reactions, different sub-oxides exhibit layered spatial distribution characteristics. From the distribution of $O_2$in Figure 4(a), it can be seen that the pattern of oxygen consumption in the flow field closely matches the distribution of suboxides, indicating that oxygen is greatly consumed during the combustion process and that its consumption process is closely related to the formation of suboxides. The oxygen concentration gradually decreases in the flow field, while the concentration of suboxides continues to rise with the progression of the combustion reaction. This phenomenon conforms to the basic law of reactant consumption and product formation.

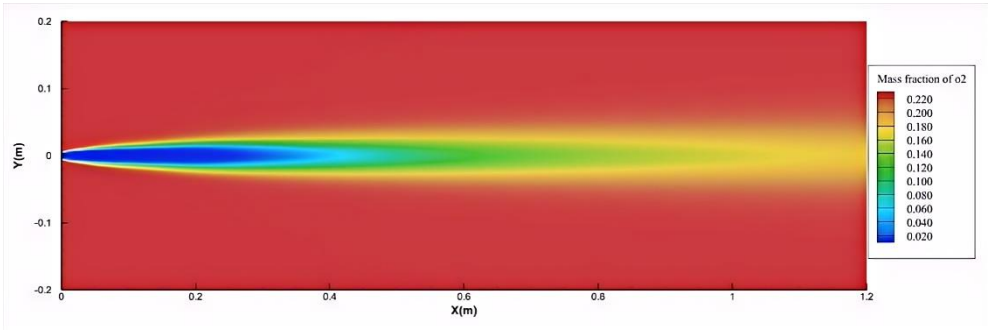


*(a)Mass fraction of $O_2$*

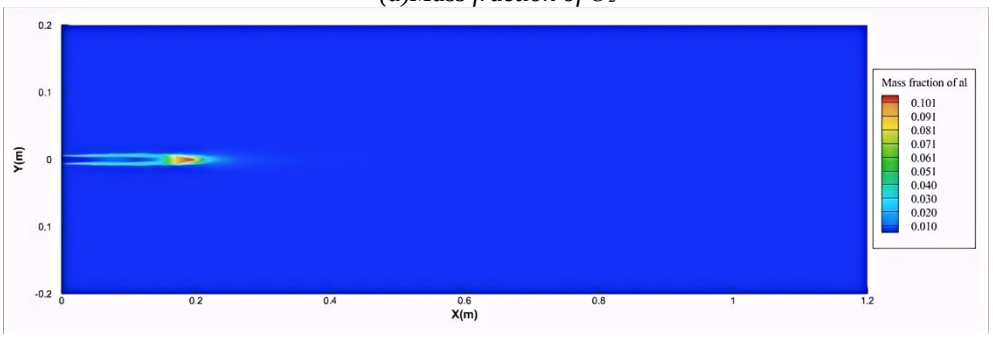


*(b)Mass fraction of Al*

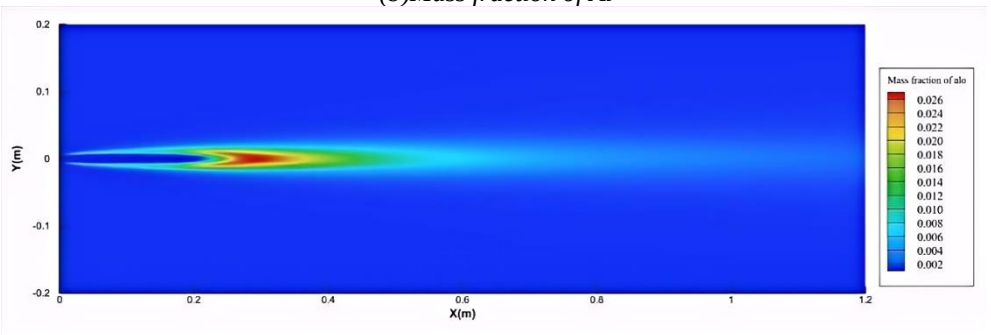


*(c)Mass fraction of $Al_2O_3$*

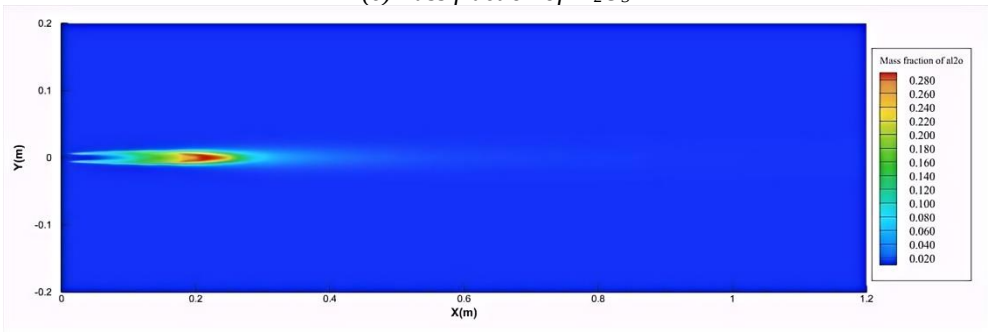


*(d)Mass fraction of $Al_2O$*

ISSN 2616-5767 Vol.9, Issue 3: 1-14, DOI: 10.25236/AJETS.2026.090301

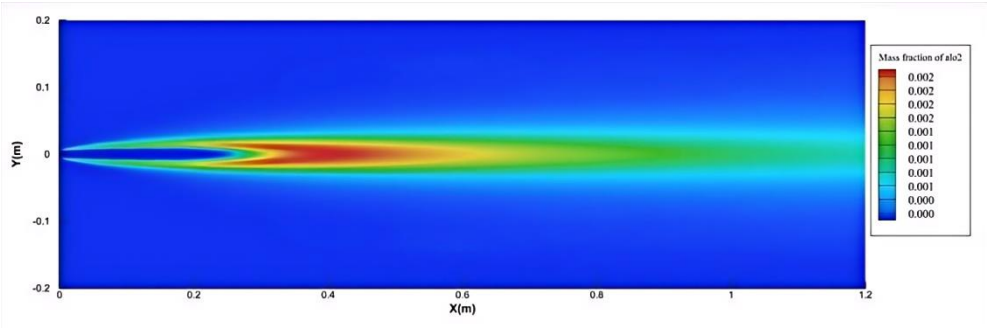


*(e)Mass fraction of $AlO_2$*

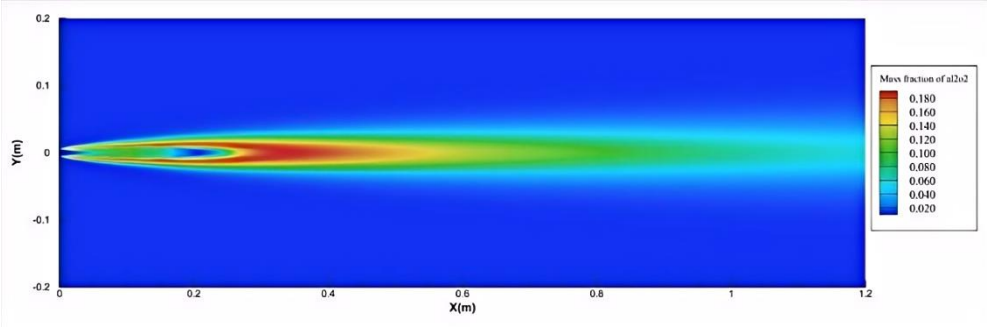


*(f)Mass fraction of $Al_2O_2$*

*Figure 4: Key Gas Phase Component Mass Fraction Distribution Map.*

### *4.2. Flow Field Temperature Distribution and Flame Structure Characteristics*

Figure 5(a) shows the temperature distribution cloud map of the flow field and the streamline distribution after the combustion of 400 nm aluminum particles reaches a stable state. The temperature distribution of the flow field is highly consistent with the distribution characteristics of the various components of aluminum gas-phase combustion, indicating that the combustion process of aluminum particles in the flow field is closely related to the oxidation reaction of gaseous suboxides with oxygen. The large amount of heat released by the oxidation reaction of suboxides forms a significant temperature gradient, and the area of highest temperature highly coincides with the distribution region of gaseous aluminum components, which means that the reaction between suboxides and oxygen in this area is more intense, and the intense heat release ultimately forms a high-temperature core region. Affected by the convection of heated air, the temperature gradient along the radial direction of the Y-axis decays rapidly, keeping the flame width stable. Generally speaking, the flame width is closely related to the particle size of aluminum: the smaller the particle size, the faster the particles are heated by the hot gas, and the earlier the evaporation of the gaseous aluminum components begins. This pattern has also been confirmed by numerical results. In the downstream region of the axial temperature distribution, the incompletely reacted sub-oxides come into contact with oxygen and undergo afterburning, causing the high-temperature region to extend a certain distance along the airflow direction, and then the temperature gradually approaches the co-flowing air temperature.

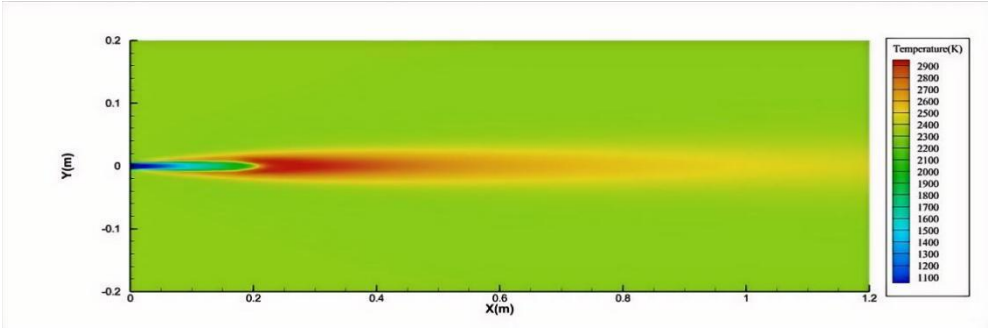


*(a)*

ISSN 2616-5767 Vol.9, Issue 3: 1-14, DOI: 10.25236/AJETS.2026.090301

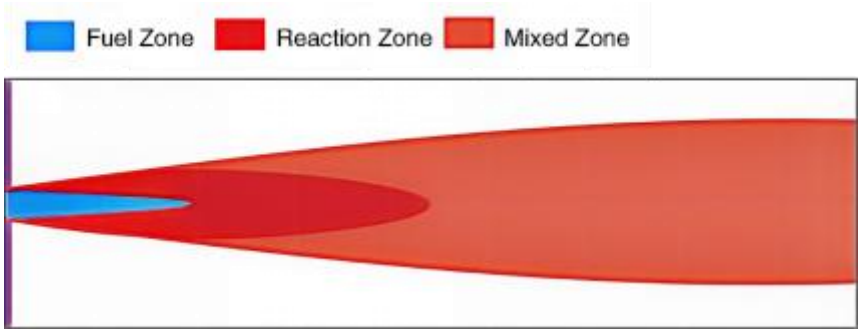


*(b)*

*Figure 5: Temperature and Streamline Distribution of the Combustion Flow Field*

Based on the distribution characteristics of temperature in the flow field and the evolution patterns of gas-phase components, the structure of the aluminum particle-air jet flame can be divided into three typical regions. As shown in Figure 5(b): 1) Fuel zone: located in the core area of the jet, it is the initial distribution area of aluminum particles carried by the carrier gas 2) Reaction zone: located outside the fuel zone, it is the high-temperature core area where gaseous aluminum and suboxides produced by the evaporation of aluminum particles undergo intense gas-phase combustion with oxygen 3)Mixing Zone: Located at the outermost part of the reaction zone, it is the area where incompletely reacted suboxides mix further with the oxygen in the surrounding air and undergo afterburning.

The regional division of the above flame structure clearly reveals the spatial evolution characteristics of the combustion of aluminum particle clusters, laying the foundation for subsequent analysis of the generation locations and coalescence evolution patterns of alumina particles.

### *4.3. Granular Phase*

Figure 6(a) compares the axial temperature distribution patterns of aluminum particles with three particle sizes of 200 nm, 400 nm, and 600 nm. It can be seen from the figure that particle size has a significant impact on the trend of combustion temperature: the temperature curve of 200 nm particles rises rapidly within a short axial distance and reaches a peak, while the heating process of 600 nm particles is more gradual, and the peak position shifts noticeably backward. Specifically, the temperature peak of 200 nm particles appears near $X \approx 0.2$ m, the peak of 400 nm particles is located at $X \approx 0.24$ m, and the peak of 600 nm particles shifts to $X \approx 0.3$ m. The fundamental reason for this phenomenon is that smaller particles have a higher specific surface area, and under the same heat flow conditions, their evaporation rate is faster. It is noteworthy that the temperature of particles of all sizes gradually decreases with increasing axial distance after reaching their peak. However, due to the transport effects of the flow field, incompletely burned gaseous aluminum and sub-oxides are carried to the downstream area, where their ongoing oxidation reactions release heat, allowing the downstream region to still maintain a relatively high temperature level. Figure 6(b) compares the axial distribution patterns of the number density of alumina particles generated from the combustion of aluminum particles with diameters of 200 nm, 400 nm, and 600 nm. As can be seen from the figure, particle size has a significant impact on the evolution characteristics of alumina particle number density: the alumina number density curve for 200 nm particles rises rapidly and reaches a peak within a short axial distance, then drops sharply; in contrast, the rise and fall process of 600 nm particles is more gradual, and the peak position is noticeably delayed. The peak number density of 200nm particles is about 1.125 times that of 400nm particles and about 1.365 times that of 600nm particles. It can be seen that there are significant differences in the number density distribution of alumina particles generated by the combustion of aluminum particles of different sizes. The smaller the particle size, the higher the number concentration of the product particles. Figure 6(c) shows the axial evolution of the geometric standard deviation of alumina particles produced from the combustion of aluminum particles with diameters of 200 nm, 400 nm, and 600 nm. It can be seen from the figure that particle size has a significant impact on the evolution characteristics of the geometric standard deviation: the geometric standard deviation curve of 200 nm particles rises rapidly within a shorter axial distance and reaches a peak, while the rise of 600 nm particles is more gradual, and the peak position is significantly shifted backward. Within the axial distance $X < 0.2$ m, the aluminum particles have not reached the ignition temperature, and no alumina particles are generated; therefore, the geometric standard deviation is undefined. When the axial distance $X \approx 0.2$ m, the aluminum particles were successfully ignited, and alumina particles began to form in large quantities. In the initial stage of particle formation, under the combined effects of nucleation and coagulation, the geometric standard

ISSN 2616-5767 Vol.9, Issue 3: 1-14, DOI: 10.25236/AJETS.2026.090301

deviation of particle volume increased rapidly. Subsequently, it tends to stabilize. We can observe that the alumina particles generated by the combustion of aluminum particles of different sizes have geometric standard deviations that tend to converge to a consistent stable value (about 1.8 – 2.0) in the later stages of evolution, a phenomenon that is consistent with the self-preserving distribution theory of aerosol systems [19].

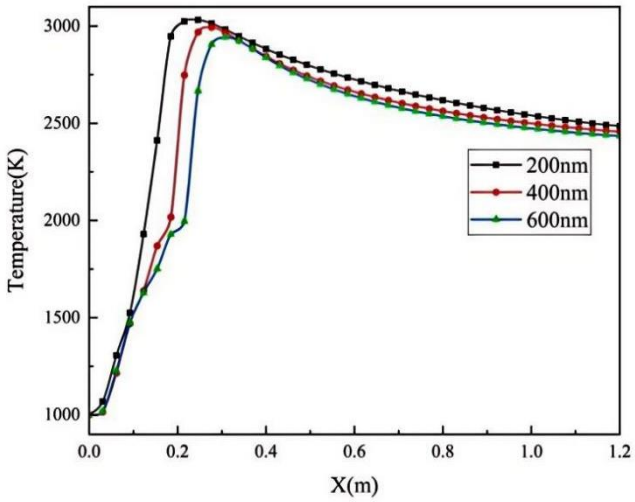


*(a)Temperature*

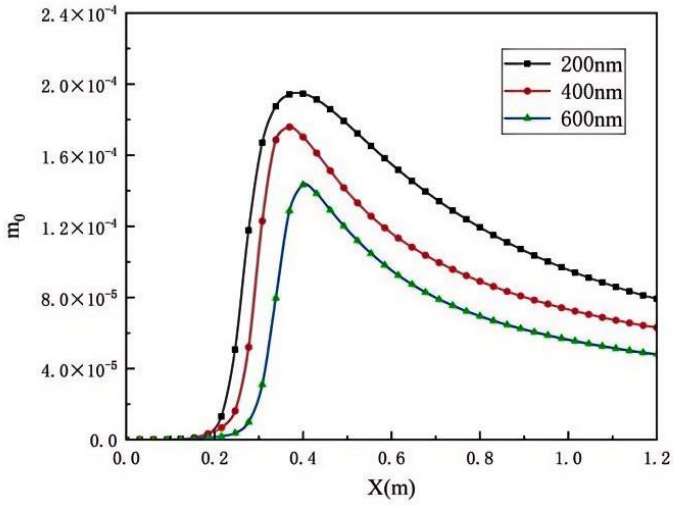


*(b)Alumina particle number density*

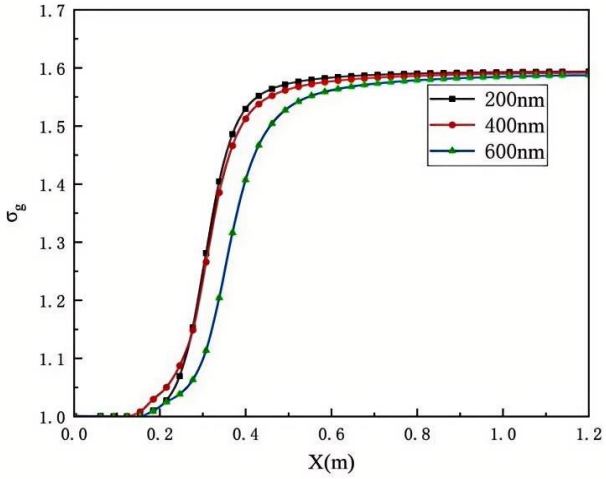


*(c)Geometric Standard Deviation*

*Figure 6: Axial distribution diagram of combustion flow field parameters for different particle size.*

ISSN 2616-5767 Vol.9, Issue 3: 1-14, DOI: 10.25236/AJETS.2026.090301

## 5. Conclusions

To address the problem of difficulty in accurately predicting the generation and evolution of alumina particles during the combustion of aluminum particle clusters, this paper establishes an Eulerian – Lagrangian – TEMOM multi-scale coupled numerical model. This model tracks the motion and combustion process of aluminum particles within the Euler – Lagrange two-phase flow framework, and uses the Taylor Expansion Method of Moments (TEMOM) to describe the coagulation kinetics of alumina particle populations, thereby enabling efficient prediction of the evolution of the alumina particle size distribution. Through numerical simulation of the jet combustion process of aluminum particles with different particle sizes, the combustion flow field structure and the evolution characteristics of alumina particle clusters were systematically analyzed. The main conclusions are as follows:

(1) The TEMOM method was introduced within the Euler – Lagrange two-phase flow framework to describe the dynamics of particle groups, achieving efficient prediction of the evolution of alumina particle size distribution. The model can simultaneously describe the evaporation and combustion of aluminum particles and the nucleation and coagulation processes of alumina particles, The calculated flame temperature structure is consistent with the results in the existing literature, verifying the reliability of this method in the simulation of metal particle combustion.

(2) The particle size of aluminum has a significant impact on the combustion structure. Small-diameter particles have higher evaporation rates and earlier ignition locations, while as the particle diameter increases, the peak flame temperature moves downstream along the axis, and the reaction zone width gradually increases, indicating that there is a significant scale effect in the combustion process of aluminum particle groups.

(3) The number density of alumina particles along the axial direction shows an evolutionary pattern of first increasing and then decreasing, and its change is mainly controlled by the competitive mechanism between gas-phase nucleation and particle coagulation. The geometric standard deviation of particle volume tends to stabilize in the later stages of evolution (about 1.8 – 2.0), showing typical characteristics of a self-preserving particle size distribution. The research results provide a theoretical reference for the optimization of propellant aluminum powder particle size and the suppression of engine deposits.

## References

*[1] Li, C., Hu, C., Xin, X., Li, Y., & Sun, H. (2016). Experimental study on the operation characteristics of aluminum powder fueled ramjet. Acta Astronautica, 129, 74-81.*
*[2] Ao, W., Fan, Z., Liu, L., An, Y., Ren, J., Zhao, M., ... & Li, L. K. (2020). Agglomeration and combustion characteristics of solid composite propellants containing aluminum-based alloys. Combustion and Flame, 220, 288-297.*
*[3] Najjar, F. M., Ferry, J. P., Haselbacher, A., & Balachandar, S. (2006). Simulations of solid-propellant rockets: Effects of aluminum droplet size distribution. Journal of Spacecraft and Rockets, 43(6), 1258-1270.*
*[4] Law, C. K. (1973). A simplified theoretical model for the vapor-phase combustion of metal particles. Combustion Science and Technology, 7(5), 197-212.*
*[5] Finke, J., & Sewerin, F. (2024). A population balance approach for predicting the size distribution of oxide smoke near a burning aluminum particle. Combustion and Flame, 265, 113464.*
*[6] Altman, I., & Pantoya, M. (2022). Comprehending metal particle combustion: a path forward. Propellants, Explosives, Pyrotechnics, 47(7), e202200040.*
*[7] Finke, J., & Sewerin, F. (2023). Combining a population balance approach with detailed chemistry to model the condensation of oxide smoke during aluminum combustion in spatially homogeneous reactors. Combustion and Flame, 248, 112510.*
*[8] Moussa, R. B., Proust, C., Guessasma, M., Saleh, K., & Fortin, J. (2017). Physical mechanisms involved into the flame propagation process through aluminum dust-air clouds: A review. Journal of Loss Prevention in the Process Industries, 45, 9-28.*
*[9] Marchisio, D. L., Vigil, R. D., & Fox, R. O. (2003). Quadrature method of moments for aggregation – breakage processes. Journal of colloid and interface science, 258(2), 322-334.*
*[10] Najjar, F. M., Ferry, J. P., Haselbacher, A., & Balachandar, S. (2006). Simulations of solid-propellant rockets: Effects of aluminum droplet size distribution. Journal of Spacecraft and Rockets, 43(6), 1258-1270.*
*[11] Zhu, M., Chen, X., Zhou, C. S., Xu, J. S., & Musa, O. (2020). Numerical study of micron-scale*

ISSN 2616-5767 Vol.9, Issue 3: 1-14, DOI: 10.25236/AJETS.2026.090301

*aluminum particle combustion in an afterburner using two-way coupling CFD–DEM approach. Flow, Turbulence and Combustion, 105(1), 191-212.*
*[12] Zhu, M., Chen, X., Zhou, C. S., & Xu, J. S. (2019). Experimental and numerical study of a full-size direct-connect dual-inlet DRE with a fuel-rich metalized solid propellant. International Journal of Heat and Mass Transfer, 140, 965-977.*
*[13] Ramkrishna, D. (2000). Population balances: Theory and applications to particulate systems in engineering. Elsevier.*
*[14] Yu, M., & Lin, J. (2009). Taylor-expansion moment method for agglomerate coagulation due to Brownian motion in the entire size regime. Journal of Aerosol Science, 40(6), 549-562.*
*[15] Bazyn, T., Krier, H., & Glumac, N. (2007). Evidence for the transition from the diffusion-limit in aluminum particle combustion. Proceedings of the Combustion Institute, 31(2), 2021-2028.*
*[16] Zou, X., Wang, N., Wang, J., Feng, Y., & Shi, B. (2021). A numerical investigation on heterogeneous combustion of aluminum nanoparticle clouds. Aerospace Science and Technology, 112, 106604.*
*[17] Zou, X., Wang, N., Liao, L., Chu, Q., & Shi, B. (2020). Prediction of nano/micro aluminum particles ignition in oxygen atmosphere. Fuel, 266, 116952.*
*[18] Zou, X., Wang, N., Wang, J., Wang, C., Han, L., & Shi, B. (2022). Numerical study on the characteristics of a nano-aluminum dust-air jet flame. Aerospace Science and Technology, 121, 107304.*
*[19] Swift, D. L., & Friedlander, S. (1964). The coagulation of hydrosols by Brownian motion and laminar shear flow. Journal of colloid science, 19(7), 621-647.*